DARPA/ONR Grant #N00014-91-J-1976

Third Quarterly Progress Report
(covering the period of February 1 - April 30, 1992)

Project Title: Development of Ultra-Low Noise, High Sensitivity Planar Metal Grating Coupled AlGaAs/GaAs Multiquantum Well IR Detectors for Focal Plane Array Staring IR Sensor Systems

Submitted to

Max N. Yoder
Office of Naval Research
Code 1114 SS
800 North Quincy Street
Arlington, VA 22217-5000

Prepared by

Prof. Sheng S. Li

Dept. of Electrical Engineering
University of Florida
Gainesville, Florida 32611

Tel.(904)-392-4937
Fax(904)-392-8671

May 1, 1992

3rd Quarterly Progress Report: February 1 - April 30, 1992

Project Title: Development of low-noise high-detectivity planar metal grating coupled III-V multiquantum-well/superlattice infrared photodetectors for focal plane array (FPA) staring infrared sensor systems.

Program Manager: Max N. Yoder, Office of Naval Research, Code 1114SS,Arlington, VA 22217.

Principal Investigator: Sheng S. Li, Professor, University of Florida, Gainesville, FL 32611.

Project Objectives:

1. To develop low-noise and high-detectivity planar metal grating coupled bound-to-miniband (BTM) GaAs/AlGaAs and step-bound-to-miniband (SBTM) InGaAs/AlGaAs /GaAs quantum well infrared photodetectors (QWIPs) for 8 to 12 μm detection.

2. To develop other new types of multicolor QWIPs with broader infrared spectral response (5 to 18 μm).

3. To conduct theoretical and experimental studies of the planar metal grating-coupled structures for normal incident illumination on the BTM and SBTM QWIPs. A variety of metal grating couplers (e.g., 1-D line-grating and 2-D cross-grating) for the QWIPs will be studied in order to achieve high coupling efficiency under normal front- and back- illuminations.

4. To develop theoretical models for predicting the dark current, photocurrent, and grating coupling efficiency in various types of QWIPs to be studied in this project.

I. Introduction

In this reporting period (2-01-92 to 4-30-92), we have continued to make a significant progress towards the program goals. We have designed, fabricated and characterized several metal grating coupled bound-to-miniband (BTM) and step-bound-to-miniband (SBTM) transition QWIPs on the GaAs and InP substrates for 8 - 12 μm focal plane arrays staring infrared sensor applications. Specific tasks performed include: (1) the design and growth of several (BTM) GaAs- and (SBTM) InGaAs-based QWIP structures as well as a new type-II normal incident AlAs/AlGaAs QWIP structure by using molecular beam epitaxy (MBE) technique, (2) the design and fabrication of the 1-D (line-grating) and 2-D (cross-grating) metal grating couplers on the QWIP's with different granting periods (1.1, 3.2, 5, 7.2, and 10 μm), (3) the theoretical and experimental studies of the light coupling quantum efficiency versus grating period for the QWIP's, and (4) the theoretical and experimental studies of the dark current versus temperature and bias voltage for the BTM and SBTM QWIP's. Detailed results are discussed in Section 3.

II. Achievements and Publications

Specific accomplishments and publications are summarized as follows:

2.1 Research Accomplishments:

1. Performed experimental studies of the light coupling quantum efficiency versus grating period for the normal incident planar metal line grating coupled GaAs/AlGaAs QWIPs. A peak coupling quantum efficiency of 11 % was obtained for QWIP with a 5 μm line grating period. Five different line grating periodicities with Λ = 1.1, 3.2, 5, 7, and 10 μm were studied. A high coupling quantum efficiency was obtained for a 2-D cross grating coupler, which was better than the incidence illumination at 45 $^{\circ}$ angle.

2. Performed numerical simulation of a 2-D (cross-grating) reflecting metal grating structure formed on the QWIPs using the method of moment. The advantage of this grating structure is that the coupling of incident radiation is indepedndent of the polarization direction of the incident light. The results showed that a significant enhancement of light coupling efficiency can be obtained by using the 2-D cross grating structure

operating in the transmission as well as reflection modes. Based on the simulation results, it is possible to design and fabricate a variety of cross grating couplers with excellent coupling efficiency for different wavelengths. We plan to design and fabricate cross grating coupler structures with different grating periods on the QWIPs during the next reporting period to evaluate the coupling quantum efficiency versus grating period in these new structures.

3. Theoretical calculations of the dark current and transmission coefficient through the global miniband formed inside the quantum well with a superlattice barrier layers have been carried out as a function of temperature and bias voltage for both the BTM and SBTM QWIPs. The results revealed that dark current in both QWIPs was dominated by the thermionically assisted tunneling conduction from the heavily populated ground states in the quantum wells via the global miniband inside the quantum wells/superlattice barrier layers for T$\geq$ 60 K, whereas the resonant tunneling conduction prevailed for T $\leq$ 40 K. The thermionic emission into the continuum bands is negligible due to the high barrier height created by the superlattice barrier layer for both QWIPs. A comparison of the calculated and measured dark current values for these two QWIPs with that of the conventional GaAs MQW QWIP's was also made in this work. The measured dark currents for both QWIP's were found in good agreement with the calculated values. In addition the dark current versus dopant density in the quantum wells has also be investigated and the results will be used in the design of new BTM QWIPs to achieve optimal performance in these devices. A paper on this study submitted to the *International Conference on Narrow Gap Semiconductors* has been accepted for presentation at the University of Southampton, UK, July 19-23, 1992. Full paper will be published in the conference proceeding.

4. Demonstrated the **first** normal incident type-II QWIP's using an indirect $Al_{0.5}Ga_{0.5}As$ /AlAs system grown on [110] GaAs substrate. A broad spectral response covering 5 - 17 μm wavelength was obtained in this new QWIP's. The dark current, absorbance, and spectral response of this detector have been characterized and the results are discussed in section 3.2.

5. Dr. Li gave an **invited talk** on the *metal grating-coupled bound-to-miniband transi-*

tion III-V multiquantum well infrared photodetectors (QWIPs) at the *Innovative Long Wavelength Photodetector Workshop* held in Jet Propulsion Lab., April 7-9, 1992. His student Larry Yu also presented a paper entitled *A Normal Incident Type II QWIP Grown on [110] GaAs substrate* at the same Workshop.

6. Dr. Li and his students attended and presented two QWIPs papers at the SPIE conferences: one was held at Somerset Hilton, NJ, March 24-26, and the other was at the SPIE OE conference on *Infrared Focal Plane Arrays* at Mariott hotel in Orlando, FL, April 22-24, 1992.

2.2. Journal Papers:

1. L. S. Yu and Sheng S. Li,"A Low Dark Current, High Detectivity, Grating Coupled AlGaAs/GaAs Mulitple Quantum Well IR Detector Using Bound-to-Miniband Transition for 10 μm Detection,"Appl. Phys. Letts., 59 (11), p.1332, Sept.9, 1991.

2. L. S. Yu, Sheng S. Li, and Pin Ho "Largely Enhanced Bound-to-Miniband Absorption in an InGaAs Multiple Quantum Well with Short-Period Superlattice InAlAs/InGaAs Barrier " Applied Phys. Letts., 59 (21), p.2712, Nov. 18, 1991.

3. L. S. Yu, Y. H. Wang, Sheng S. Li and Pin Ho,"A Low Dark Current Step-Bound-to-Miniband Transition InGaAs/GaAs/AlGaAs Multiquantum Well Infrared Detector," Appl. Phys. Letts., 60(8), p.992, Feb.24, 1992.

4. L. S. Yu, S. S. Li, Y. H. Wang, and Y. C. Kao,"A Study of Grating Periodicity Dependence of Coupling Efficiency in A Normal Incident Grating-Coupled GaAs/AlGaAs Quantum Well Infrared Detector," J. Appl. Phys., submitted, March, 1992.

5. L. S. Yu, S. S. Li,and P. Ho,"A Normal Incident Type-II Quantum Well Infrared Detector Using an Indirect AlAs/$Al_{0.5}Ga_{0.5}As$ System Grown on [110] GaAs," Appl. Phys. Letts., submitted, March 1992.

2.3. Workshop and Conference Presentations

1. L. S. Yu, Sheng S. Li, and Pin Ho, " Largely Enhanced Intra-subband Absorption in a Wide InAlAS/InGaAs Quantum Well with a Short-Period Superlattice Barrier Structure,"paper presented at the *SPIE's Symposium on Quantum Wells and Superlattices*, Somerset, NJ, 23-27 March,1992. Paper to be appeared in the conference proceeding.

2. Sheng S. Li and L. S. Yu, "Grating Coupled Bound-to-Miniband Transition III-V Quantum Well Infrared Detectors," **invited paper**, presented at *the Innovative Long Wavelength Infrared Photodetector Workshop*, Jet Propulsion Lab., Pasadena, CA, April 7-9, 1992.

3. L. S. Yu and Sheng S. Li,"A Normal Incident Type-II Quantum Well Infrared Detector Using an Indirect AlAs/$Al_{0.5}Ga_{0.5}As$ System Grown on [110] GaAs, paper presented at *the Innovative Long Wavelength Infrared Photodetector Workshop*, Jet Propulsion Lab., Pasadena, CA, April 7-9, 1992.

4. L. S. Yu, Sheng S. Li, Y. H. Wang, and P. Ho," Grating Coupled III-V Quantum Well Infrared Detectors Using Bound-to-Miniband Transition," paper presented at *the SPIE Conference on Infrared Detectors and Focal Plane Arrays at OE/Aerospace Sensing 92*," Orlando, FL, April 20-24, 1992. Full paper to be published in the conference proceeding.

5. Sheng S. Li, M. Y. Chuang and L. S. Yu,"Current Conduction Mechanisms in Bound-to-Miniband Transition III-V Quantum Well Infrared Photodetectors," paper accepted for presentation at the *International Conference on Narrow Gap Semiconductors*, University of Southampton, Southampton, UK, July 19-23, 1992

2.4 Interactions with Industrial Research Laboratories

1. Continued to collaborate with Dr. Pin Ho of General Electric Co., in Syracuse, NY, on growth of the III-V QWIP's structures for us by the molecular beam epitaxy (MBE) technique. The results so far have produced several journal and conference papers.

New QWIP samples have been grown recently, and the new devices will be fabricated and characterized in the next reporting period for comparison.

2. Continued to collaborate and exchange technical information on QWIP's research with Dr. Barry Levine of A T & T Bell Laboratories. Dr. Li and his student, L. Yu, visited Dr. Levine at A T & T Bell Lab, Murray Hill, on March 20, giving a siminar and touring their IR detector measurement facilities, and discussed with Dr. Levine and his colleaques on the QWIPs research.

3. Dr. Li's student, Larry Yu visited Martin Mariatta Laboratories, Baltimore, MD, giving a siminar there, and exchanged technical information with T. Faska and W. Beck on the BTM transition GaAs/AlGaAs QWIPs developed at UF.

III. Technical Results and Discussion

3.1 A grating coupled step-bound-to-miniband transition InGaAs/AlGaAs/GaAs quantum well infrared photodetector

ABSTRACT

A low dark current metal grating coupled step-bound-to-miniband (SBTM) transition quantum well infrared photodetector (QWIP) using a lightly strained $In_{0.07}Ga_{0.93}As$ quantum well with a short-period $Al_{0.4}Ga_{0.6}As$ -GaAs superlattice barrier structure has been developed. The new structure created a potential 'step' in the superlattice barrier to block the undesirable electron tunneling current from the heavily doped ground state in the quantum well which results in a significant reduction in the device dark current. The measured absorbance spectra and photocurrent are in good agreement with our theoretical predictions. The responsivity R_λ at V_b = 6 V and T = 77 K was found equal to 0.2, 0.15 A/W for the backside, and front normal incident illumination, respectively.

3.1.1 INTRODUCTION

Most of the work reported in the literature on III-V quantum well long wavelength infrared photodetectors (LWIPs) has been focused on the lattice-matched narrow well width

GaAs/AlGaAs quantum well systems [1-8]. Recent studies[9-11] revealed that infrared detectors for 8 - 12 μm detection may be obtained by using an enlarged multiquantum well/superlattice barrier structure and resonant tunneling mechanisms. A significant improvement in the intersubband absorption and thermionic emission property has been successfully demonstrated using the GaAs/AlGaAs superlattice reinforced bound-to-miniband (BTM) transition structure. The replacement of bulk barrier region with a very short period superlattice barrier layer offers several new properties such as reduction of interface recombination, elimination of deep-level defect related phenomena[12], realization of a new type of quantum photocurrent gain ($\sim 10^4$)[11,13], and a significant enhancement of intersubband absorption[10].

Due to the limitation of selection rule[14], there has been some interest in proposing a linear edge illumination tilted at 45°[1-8] and/or the phase modulated reflection metal grating coupled quantum well infrared photodetectors (QWIPs) using a backside[15-17] illumination on LWIPs. Recently, we have reported an amplitude modulated metal grating coupled AlGaAs/GaAs QWIP using a two-dimensional (2-D) front normal illumination[9,18,19]. A thin (0.1 μm) metal grating contact structure is formed on the detector surface to serve both as a large area infrared coupler and as an effective top ohmic contact. By using a 5 μm grating periodicity, a peak detectivity $D^* = 1.6 \times 10^{10}$ cm$\sqrt{Hz}$/W was obtained at $\lambda_p = 8.9$ μm and T = 77 K with front normal illumination. This simple but extremely uniformed planar grating coupler structure is indeed very favorable for the large area focal plane arrays and infrared image sensors applications.

Additional advantages of using planar metal grating coupled structure in the QWIPs include: (1) enabling an efficient coupling of the normal incident IR radiation into the quantum wells of the QWIP, (2) eliminating the undesirable cross-talk in the detector arrays and clearing the infrared image from the effect of multiple (ghost) images, (3) offering an extremely thin and smooth surface quality, which is essential for surface passivation and antireflection coatings, (4) no extra epitaxial layer growth is needed for forming the dielectric grating by chemical or dry etchings, and (5) the metal grating coupler is simple and easy to fabricate, and is compatible with the GaAs LSI technology. Therefore, low cost, high yield, and large area long wavelength infrared image sensors and focal plane arrays can be readily fabricated using the metal grating coupled III-V multiquantum well LWIPs.

In this paper we report a planar metal grating coupled ultra-low dark current LWIP by using lightly-strained step-bound-to-miniband (SBTM) transition InGaAs/GaAs/AlGaAs quantum well structure. As illustrated in figure 1, the transition scheme for the SBTM LWIP's is from the localized bound ground state in the enlarged $In_{0.07}Ga_{0.93}As$ (106Å) quantum well to the resonant-coupled miniband of GaAs/$Al_{0.4}Ga_{0.6}As$ superlattice (SL) barrier. This new structure created a potential 'step' in the superlattice barrier region to block the undesirable tunneling dark current from the heavily doped ground state E_{EW} in the quantum well. The physical parameters of the quantum wells and superlattices are chosen so that the ground bound state in the enlarged (EW) InGaAs well is pushed below the step barrier, and the first excited level E_{EW_1} of the quantum well is merged and lined up with the ground level of the miniband E_{SL} in the superlattice barrier layer to achieve a large oscillation strength f and intersubband absorption coefficient α. Since the superlattice has a relatively thin barrier, the photoexcited electrons can easily tunnel through the superlattice barrier layer and transport along the aligned miniband, which are then collected by the external ohmic contacts.

3.1.2 THEORY AND EXPERIMENT

To characterize the SBTM transition we performed theoretical calculations of the energy states E_{EW}, E_{SL} and the transmission coefficient T^*T on our LWIP's by using the multiple-layer transfer matrix method[18], and the results are shown in figure 2. It is noted that a broad and strongly degenerated miniband E_{SL} was formed inside the enlarged well by using the superlattice barrier structure. The ground state of the enlarged InGaAs well is confined much below the step barrier height so as to reduce the sequential tunneling and hopping currents. As a comparison, in the inset of figure 2, we calculated the transmission coeffecient of the superlattice for both the step-bound-to-miniband (SBTM) and the normal bound-to-miniband (BTM) transition structure without the potential step. Many orders of magnitude reduction in T^*T were observed in the present SBTM structure.

The SBTM detector structure was grown on a semi-insulating (S.I.) GaAs substrate by using the molecular beam epitaxy (MBE) technique. A 1 μm thick GaAs buffer layer of 1.4×10^{18} cm^{-3} was first grown on a S.I. GaAs substrate, followed by the growth of a 40-period of $In_{0.07}Ga_{0.93}As$ quantum wells with a well width of 106 Å and a dopant

density of 1.4×10^{18} cm^{-3}. The barrier layer on each side of the quantum well consists of a 5-period of undoped $Al_{0.4}Ga_{0.6}As$ (30 Å) /GaAs (59 Å) superlattice layers which were grown alternatively with the InGaAs quantum wells. Finally, an n^+-GaAs cap layer of 0.4 μm thick and dopant density of 1.4×10^{18} cm^{-3} was grown on top of the MQW/SL layer structure to facilitate ohmic contacts. An array of 200×200 μm^2 mesas were chemically etched down to n^+-GaAs buffer contact layer on the GaAs substrate. Finally, AuGe/Ni/Au ohmic contacts were evaporated onto the top and bottom of n^+-GaAs contact layers by using E-beam evaporation.

Device characterization was performed in a liquid-helium cryogenic dewar. An HP4140B semiconductor parameter analyzer was used to measure the dark current vs. voltage (I-V) curves. Under dark conditions, electrons can transfer out of the quantum wells and produce the observed current mainly via two mechanisms. One is attributed to the thermionic emission out of the quantum wells, which is the dominant current component at higher temperatures (i.e., for $T \geq 77$ K). The other is the thermally generated carriers tunneling through the superlattice miniband. In the present SBTM transition LWIP structure, we created a levitated potential step in the superlattice to block much of the tunneling current component due to electron tunneling from the heavily populated ground state at low temperatures. We also chose a high value of 'Al' composition, $x = 0.4$, which gave rise to a barrier potential as high as $\Delta E_c \simeq 388$ meV ($\sim 65\% \Delta E_g$), to suppress the thermionic emission out of the quantum wells. Figure 3 shows the measured dark I-V curves for temperatures between 35 and 92 K. Substantial reduction in device dark current was achieved in the present step-potential reinforced InGaAs multiquantum well/GaAs/AlGaAs superlattice barrier structure. To identify the origins of the dark currents flow in the detector we performed the numerical calculation of the dark currents using the expression[21,9]

$$I_D = \frac{4\pi q A v(\mathcal{E}) m^* kT}{h^2 L} \int_0^\infty |T(E,\mathcal{E})|^2 \{ln[1 + e^{-(E-E_f)/kT}] - ln[1 + e^{-(E-qV-E_f)/kT}]\} dE; \quad (1)$$

where $v(\mathcal{E})$ is the electron velocity in GaAs which is given by[22]

$$v(\mathcal{E}) = \frac{\mu\mathcal{E} + v_s(\mathcal{E}/\mathcal{E}_0)^4}{1 + (\mathcal{E}/\mathcal{E}_0)^4} \quad (2)$$

where q is the electron charge, A is the device area, m^* is the electron effective mass, L is the multiquantum well period, E_f is the Fermi level, $\mathcal{E}_0$ is the critical field which is equal

to 4×10^3 V/cm for GaAs. As previously described[18], the parameter $|T(E,\mathcal{E})|^2$ is the field-dependent transmission coefficient which can be calculated by using the multi-layer matrix method, assuming the potential energy variation of $V(x) = V_0 + q\mathcal{E}x$. The calculated current values are in good agreement with the observed results, which shows that the levitated step potential barrier is indeed very effective in suppressing the device dark current. Another interesting result observed in this SBTM LWIP's (as shown in figure 3) is the negative resistance exhibited by the sequential resonant tunneling through an expanding high-field superlattice domain[3] at T = 35 K.

The intersubband absorption measurements for the present detector were performed at 300 K using a Perkin-Elmer Fourier transform infrared (FTIR) spectroscopy. Figure 4 shows the room temperature absorption spectra at the Brewster's angle ($\theta_B = 73°$). The measured peak absorbance A = -$\log_{10}$ [transmission] was found to be about 40 mAbs. The absorption peak is centered at 11.4 μm. The full width at half-maximum (FWHM) of the absorption peak is about 220 cm^{-1}.

To facilitate the top normal incidence of infrared light, we developed a planar metal grating coupler which consists of regularly spaced metal grating strips deposited on top of the detector. It is assumed that the metal strips in the grating contact structure (Figure 1) have a large conductivity σ and a negligible thickness ($h \rightarrow 0$). The metal is equivalent to a lossy dielectric with relative permittivity $\epsilon = 1 + i\sigma/\epsilon_o\omega$. When an infrared light is impinging normally upon the grating surface, the corresponding transmission magnetic field in the GaAs/AlGaAs quantum well region can be expressed by[22]

$$H_t(y,z) = T_0 e^{ikz} + \sum_{m=1}^{\infty} T_m cos(8m\pi y/\Lambda) e^{i\Gamma_m z} \tag{3}$$

where T_0 is the zeroth-order transmission coefficient, Γ_m is the Gamma function of order m, and T_m ($m = 1, 2, \cdots$) is the high order transmitted wave amplitudes. The grating coupling equation for the forward-diffracted (transmitted) waves can be written as[23]

$$n_1 sin\theta_t^{(m)} = n_0 sin\theta_i - \frac{m\lambda}{\Lambda} sin\phi \tag{4}$$

where n_0 and n_1 denote the optical refractive indices of layers above and beneath the grating layer, respectively, and are given by $n_0 = \sqrt{\epsilon_0}$ and $n_1 = \sqrt{\epsilon_1}$. The cutoff periodicity Λ_c for

the mth diffracted mode for a given incident angle θ can be estimated by using the relation

$$\Lambda_c = \frac{\pm m\lambda}{\pm sin\theta_i - (\epsilon_1)^{1/2}} \qquad m = 0, 1, 2, \cdots \tag{5}$$

where λ is the incident wavelength, ϵ_1 is the dielectric constant of GaAs which is equal to 10.7. The detector's quantum efficiency η can be determined from the relation

$$\eta(\Lambda) = \frac{1}{2}\sum_m \frac{\Gamma_m |T_m(\Lambda)|^2}{2k}\{1 - e^{-\alpha[\theta_t^{(m)}(\Lambda)]L}\} \tag{6}$$

where L is the total length of the superlattice absorption region. A factor of $1/2$ in front of the summation above is included to account for the reduction of an unpolarized light source. The photocurrent responsivity R_λ of the multiquantum well LWIP can be expressed as

$$R_\lambda(\Lambda) = \eta(\Lambda) \cdot \frac{e\lambda}{hc} G, \qquad (A/W) \tag{7}$$

where e is the electronic charge; G is the photoconductive gain. The photocurrent was measured using a CVI Laser Digikrom 240 monochromator and an ORIEL ceramic element infrared source. The responsivity R_λ = 0.2, 0.15 A/W was obtained at V_b = 6 V and T = 77 K for the backside, and front normal surface illumination, respectively. Figure 5 shows the top view of the metal grating coupled QWIP's with a strip grating period of 5 μm. Figure 6 shows the relative responsivity with grating enhanced normal incident IR illumination, measured at $V_b = \pm 6V$, and T = 77 K. A peak wavelength at Λ = 10 μm was obtained in this IR detector.

3.1.3 CONCLUSION

In conclusion, we have demonstrated a new metal grating coupled step-bound-to-miniband (SBTM) transition LWIP's using a large (106 $\AA$) InGaAs multiquantum well and a short-period (59$\AA$/30$\AA$) GaAs/AlGaAs superlattice barrier layer structure and resonant tunneling mechanisms. Both the front and backside normal illuminations are allowed due to the strong coupling effects of the strip-metal grating on top of the detector. An optimum grating period of $\Lambda = 5\mu$m was used to achieve the best coupling efficiency in the spectral range of 8 - 14 μm for our SBTM LWIPs. The new SBTM transition structure provides a levitated potential 'step' in the superlattice barrier to block much of the tunneling current component from the heavily populated ground state in the enlarged quantum wells, which results in a significant

reduction of the device dark current. A peak detectivity of $D^* = 2.1 \times 10^{10} cm\sqrt{Hz}/W$ was obtained at $\lambda = 9.25$ μm and T = 63 K. With high detectivity and uniformity, this new SBTM LWIP's can be used for a wide variety of long wavelength (e.g., 8 - 12 μm) infrared applications.

3.1.4 REFERENCES

1. J. S. Smith, L. C. Chiu, S. Margalit, A. Yariv, and A. Y. Cho, J. Vac. Sci. Technol. B **1**, 376 (1983).

2. B. F. Levine, G. Hasnain, C.G. Bethea, and Naresh Chand, Appl. Phys. Lett. **54**, 2704 (1989).

3. S.D. Gunapala, B.F. Levine, R.A. Logan, T. Tanbun-Ek, and D.A. Humphrey, Appl. Phys. Lett., **57**, 1802 (1990).

4. Hiromitsu Asai and Yuichi Kawamura, Appl. Phys. Lett., **56**, 746 (1990).

5. B. F. Levine, K.K. Choi, C.G. Bethea, J. Walker, and R.J. Malik, Appl. Phys. Lett.**50**, 1092 (1987).

6. D.D. Coon and R. P. G. Karunasiri, Appl. Phys. Lett. **33**, 495 (1984).

7. B. F. Levine, G. Hasnain, C.G. Bethea, and Naresh Chand, Appl. Phys. Lett., **54**, 2704 (1989).

8. Larry S. Yu, Sheng S. Li, Y.H. Wang, and Pin Hu, Appl. Phys. Lett., **60**, 992 (1992).

9. K. K. Choi, B. F. Levine, R. J. Malik, J. Walker, and C.G.Bethea, Phys. Rev. **B 35**, 4172 (1987).

10. A. Kastalsky, T. Duffield, S.J. Allen, and J. Harbison, Appl. Phys. Lett. **52**, 1320 (1988).

11. P. F. Yuh and K. L. Wang, Appl.Phys. Lett. **65**, 4377 (1989).

12. B. K. Janousek, M.J. Daugherty, W. L. Bloss, M. L. Rosenbluth, M. J. O'Loughlin, H. Kanter, F.J. De Luccia, and L.E. Perry, J. Appl. Phys.**67**, 7608 (1991).

13. Larry.S. Yu and Sheng S. Li, Appl. Phys. Lett. **59**, 1332 (1991).

14. Larry S. Yu, Sheng S. Li,and Pin Hu, Appl. Phys. Lett.**59**, 2712 (1991).

15. S. S. Li, Y.H. Wang, Larry S. Yu, S. Zhu, R. M. Park and Y.W. Lin *International Electron Devices and Materials Symposium*, Nov. 14 -16, Hsinchu, Taiwan (1990).

16. H. Sakaki, M. Tsuchiya, and J. Yoshino, Appl. Phys. Lett., **47**, 295 (1985).

17. F. Capasso, K. Mohammed, A.Y. Cho, R. Hull, A.L. Hutchinson, Appl. Phys. Lett. **47**, 420 (1985).

18. L. C. West and S. J. Eglash, Appl. Phys. Lett. **46**, 1156 (1985).

19. K. W. Gossen and S.A. Lyon, Appl. Phys. Lett., **53**, 1027 (1988).

20. G. Hasnain, B. F. Levine, C. G. Bethea, R.A. Logan, J. Walker, and R. J. Malik, Appl. Phys. Lett., **54**, 2515 (1989).

21. Andersson, L. Lundqvist, and Z.F. Paska, Appl. Phys. Lett.,**59**, 859 (1991).

22. Larry S. Yu, Sheng S. Li, Y.C. Kao, *Proc. Government Microcircuit Applications Conference*, Nov. 6 -8, Las Vegas, p.479 (1990).

23. Larry S. Yu, Sheng Li, Y.H. Wang, and Pin Ho, *to be published in* J. Appl. Phys., Feb., 1992.

24. B. F. Levine, C.G. Bethea, G. Hasnain, V.O. Shen, E.Pelve, R.R. Abbott, and S.J. Hsieh, Appl. Phys. Lett. **56**, 851 (1990).

25. R. Tsu and L. Esaki, Appl. Phys. Lett. **22** 562 (1973).

26. S.M. Sze, *High-Speed semiconductor Devices*, John Wiley & Sons, pp. 60 (1990).

27. G. Hasnain, B.F. Levine, S. Gunapala, and Naresh Chand, Appl. Phys. Lett. **57**, 605 (1990).

28. Larry. S. Yu, S. S. Li, Y. C. Kao, *Proc. International Electron Devices and Materials Symposium*, Nov.14 -16, Hsinchu, Taiwan, p.468 (1990).

29. B.F. Levine, A.Y. Cho, J. Walker, R.J. Malik, D.A. Kleinman, and D.L. Sivco, Appl. Phys. Lett., **52**, 1481 (1988).

30. Larry S. Yu, Sheng S. Li, and Pin Ho, Appl. Phys. Lett., 59(21), p.2712, (1991).

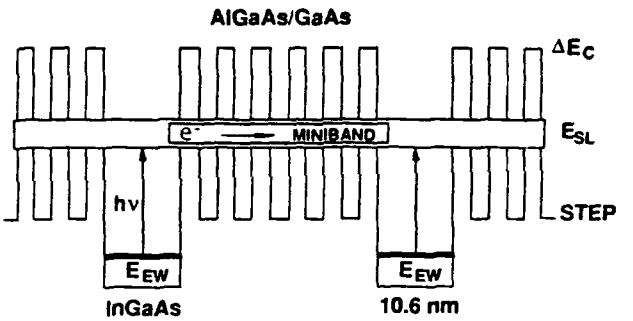

FIG. 1. The schematic energy-band diagram for the step-bound-to-miniband (SBTM) transition in a new LWIPs structure. A potential step is created in the GaAs/AlGaAs superlattice barrier layer to suppress the tunneling current from the heavily populated ground state in the InGaAs quantum well.

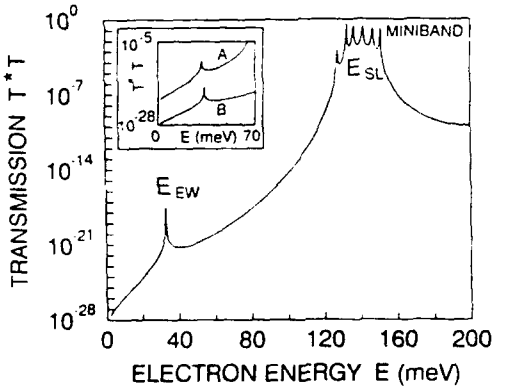

FIG. 2. The calculated quantized energy states and transmission coefficient T^*T for the present SBTM transition structure. Inset: The calculated T^*T for a SBTM (curve B) and a BTM (curve A) LWIP's.

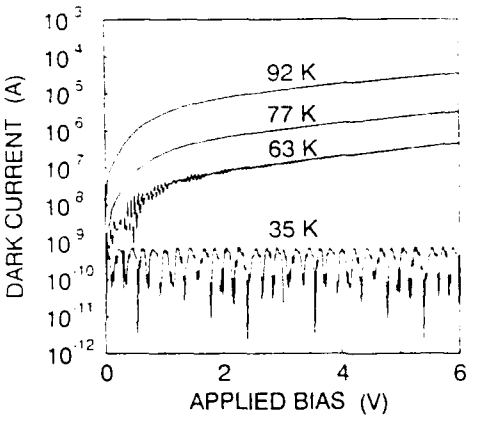

FIG. 3. Measured dark current vs applied bias for a SBTM LWIPs for $35 < T < 92$ K. Note that the dark current is dominated by thermionic emission for $T > 77$ K and by sequential tunneling for $T < 50$ K.

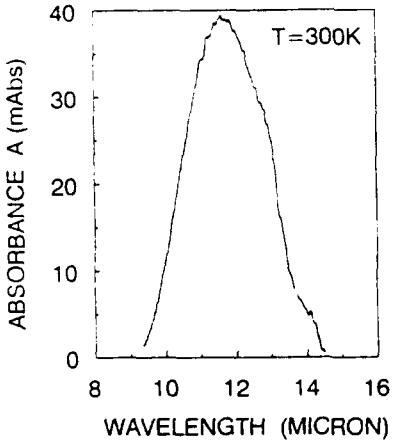

FIG. 4. Measured room-temperature ($T = 300$ K) intersubband absorbance vs wavelength for the SBTM LWIPs by FTIR spectroscopy at Brewster's angle.

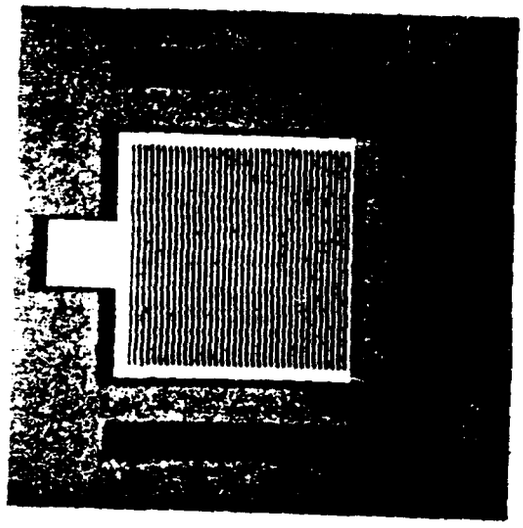

Figure 5 *Top view of a metal grating coupled SBTM LWIP's, with a 5 μm grating period.*

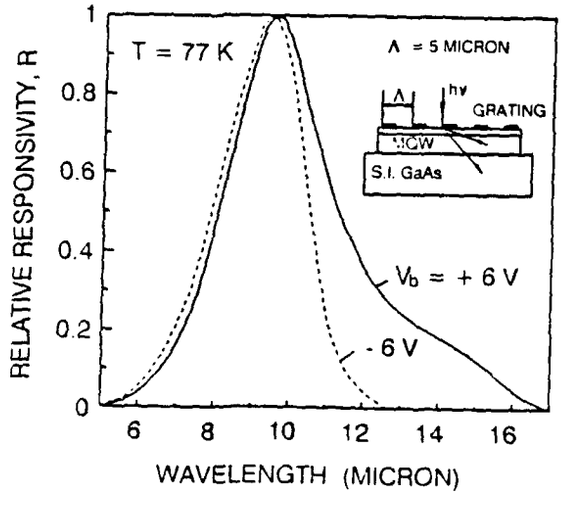

Figure 6 Relative responsivity versus wavelength for a grating coupled SBTM LWIP's, measured at $V_b = \pm 6$ V, and T = 77 K.

3.2 A normal incidence type-II quantum well infrared photodetector using an indirect $AlAs/Al_{0.5}Ga_{0.5}As$ system grown on [110] GaAs

ABSTRACT

The first *type-II* indirect $AlAs/Al_{0.5}Ga_{0.5}As$ quantum well long wavelength infrared photodetector (LWIP's) is demonstrated. A *normal incident excitation* of long wavelength intersubband transition is achieved in the [110] X-band confined AlAs quantum wells. The peak wavelength of the detector is found to be at $\lambda_p = 12.8$ μm with its spectral sensing range extended from 5.6 to 18 μm.

3.2.1 INTRODUCTION

Most work on quantum well infrared photodetectors (QWIPs) has been focused on type-I direct and conventional Γ-band GaAs quantum well structures[1-9] grown on GaAs [001] direction, in which the shapes of constant energy surfaces are isotropic with spherical symmetry. In this type of structure, due to the selection rule[1,3,6], only the component of IR radiation with electric field $\vec{\mathcal{E}}_\perp$ *vector perpendicular to the quantum well layers* will give rise to intersubband transition in the quantum wells. No intersubband infrared absorption in the quantum wells is expected in the ordinarily bare surface at normal incidence. In general, a grating coupler[5] or 45 $^\circ$ incidence [2] is required to induce the perpendicular electric field component for intersubband resonance. Recently[10-12], we have successfully demonstrated high performance quantum well infrared detectors by using a top surface strip metal-grating coupler for normal incidence. We have also found that the infrared coupling efficiency is strongly grating-period dependence. For example, for a peak wavelength of $\lambda_p = 9.8$ μm detection, a $\Lambda = 5$ μm period of strip metal (Au) grating structure produces the best coupling quantum efficiency , followed by 10, 7, and 3.2 μm. An overall quantum efficiency of 11% has been achieved in our QWIPs with a cutoff wavelength of $\lambda_c = 12.8$ μm.

Motivated by the possibility of realizing normal incidence quantum well infrared detectors without using the complex grating structures, we conducted a study of using type-II indirect III-V quantum well heterostructures for long wavelength infrared detectors. In such a system the conduction-band minimum is at the X point of the Brillouin zone (BZ). The

constant energy surface will also undergo change from a typical sphere at the zone center of direct (i.e. GaAs) to off-center ellipsoids of indirect (i.e. AlAs) gap material. For AlAs, there are six ellipsoids along [100] axes with the centers of the ellipsoids located at about three-fourth of the distance from the BZ center. By choosing a proper growth direction (i.e. [110] direction), due to the anisotropic band structures, it is possible to realize large area normal incident excitation of intersubband transitions in the type-II quantum well structures.

3.2.2 THEORY AND EXPERIMENT

In this section we report the first normal incident type-II long wavelength (5 - 18 μm) infrared photodetector using an indirect $AlAs/Al_{0.5}Ga_{0.5}As$ quantum well structure grown by molecular beam epitaxy (MBE) on [110] GaAs substrate. Unlike the typical direct type-I GaAs/AlGaAs system, we use the larger energy bandgap $AlAs$ material as the quantum well layer and $Al_{0.5}Ga_{0.5}As$ as the barrier layers. Since the compound of $Al_xGa_{1-x}As$ becomes an indirect bandgap material for $x > 0.45$, the typical conduction-band minimum would shift from Γ-band into X-band. The conduction band offset of $Al_{0.5}Ga_{0.5}As$ over the $AlAs$ is about 170 meV. Figure 1 shows a schematic conduction-band diagram for the type-II indirect $AlAs/Al_{0.5}Ga_{0.5}As$ quantum well structure, in which the electrons are confined inside the $AlAs$ layer. The intersubband transition is from the ground bound state E_0 of AlAs quantum well to the quasi-continuum state above the $AlAs/Al_{0.5}Ga_{0.5}As$ barrier.

Our sample of type-II QWIP structure was grown on a [110] GaAs substrate by using the molecular beam epitaxy (MBE) technique. A 1 μm thick n-GaAs buffer layer of $N_d = 2 \times 10^{18}\ cm^{-3}$ was first grown on a S.I. [110] GaAs substrate, followed by the growth of a 20-period of $AlAs$ quantum wells with a well width of 30 Å and doping concentration of $2 \times 10^{18}\ cm^{-3}$. The barrier layer on each side of the quantum well consists of an undoped $Al_{0.5}Ga_{0.5}As$ (500 Å) layer. Finally, an n-GaAs cap layer of 0.3 μm thick and dopant density of $2 \times 10^{18}\ cm^{-3}$ was grown on top of the MQW/SL layer structure to facilitate ohmic contacts. In the $Al_xGa_{1-x}As$ alloy system the column-III (Ga,Al) atoms and the column-V (As) atoms are placed in two separate fcc lattices displaced from each other by one-quarter of a body diagonal. The change in lattice constant from $Al_{0.5}Ga_{0.5}As$ to $AlAs$ is very small (about 0.06% at room temperature). There exists a long-range order in the crystal with the sites $0,0,0$ and $\frac{1}{2},\frac{1}{2},0$ in each unit cell preferred by Ga atoms and the sites $\frac{1}{2},0,\frac{1}{2}$ and

$0, \frac{1}{2}, \frac{1}{2}$ preferred by Al atoms. For $Al_{0.5}Ga_{0.5}As$, the structure consists of alternating AlAs and GaAs *monolayers* when viewed along the [110] growth direction.

The infrared absorption of our sample was measured at room temperature using a Perkin-Elmer Fourier transform infrared (FTIR) spectrometer[5,6,10]. Figure 2 shows the result of a room temperature absorption spectrum measurement under normal incidence. The peak absorbance mA = - 1000 log_{10}[transmission] was found to be 20 mAbs , which corresponds to a transmission reduction of $\Delta T/T = 4.5$ %. The first absorption peak is at $\lambda = 13.7\mu$m with a spectral range of 9.5 - 18 μm. The second absorption peak occurs at 7.2 μm with a spectral range of 6 - 9.5 μm, which is attributed to the higher band state transition (E_2 - E_1) of the quantum well. The results are in a good agreement with our theoretical calculations by the matrix method[6,11].

Device characterization was performed in a liquid-helium cryogenic dewar[7,10]. An HP4145 semiconductor parameter analyzer was used to measure the dark current vs. voltage (I-V) curves. Figure 3 shows the measured dark I-V curves for temperatures between 68 and 89 K. Substantial reduction in device dark current was achieved in the present type-II structure. To facilitate the normal infrared illumination, an array of 210 $\times$ 210 μm^2 mesas were chemically etched down to n^+-GaAs buffer contact layer on the GaAs substrate. Finally, AuGe/Ni/Au ohmic contact was formed on top of the sample, leaving a central sensing area of 190 $\times$ 190 μm^2 for normal illumination. The photocurrent was measured using a CVI Laser Digikrom 240 monochromator and an ORIEL ceramic element infrared source. The peak responsivity $R_p = 42$ mA/W was obtained at $V_b = 3.0$ V and T = 20 K. Figure 4 shows the normalized responsivity versus wavelength measured at T = 20 K. The peak wavelength was found at $\lambda_p = 12.8$ μm, and the spectral response range extended from 5 to 18 μm.

To understand the basics of the normally induced intersubband transitions and the corresponding indirect type-II quantum well infrared photodetectors, we start with the Hamiltonian description of quantum mechanics for an electron[13]

$$H_o = \frac{p^2}{2m} + V(\mathbf{r}) + \frac{\hbar}{4m^2c^2}\sigma \cdot (\nabla V(\mathbf{r}) \times \mathbf{p}) \tag{8}$$

where m, p, and σ are the mass, momentum, and spin operators on an electron, respectively. V($\mathbf{r}$) is a periodic potential function. The system under consideration consists of an assembly

of electrons and the infrared radiation field. The Hamiltonian of this system, $\mathcal{H}$, may be written as the sum of the unperturbed Hamiltonian $\mathcal{H}_0$ and the perturbing Hamiltonian $\mathcal{H}'$ which represents the interaction between the electrons and the incident infrared photon

$$\mathcal{H} = \mathcal{H}_o + \mathcal{H}'_{rad} \tag{9}$$

The matrix element of intersubband transition in the quantum well is given by[14,15]

$$M_{fi} = \int \varphi_{kf} H'_{rad} \varphi_{ki} d\mathbf{r} = -q(\frac{2\pi}{Vcn\hbar\omega})^{1/2} \mathbf{e}_\omega \cdot \nabla_{\mathbf{k}} \mathcal{E}_{\mathbf{k}} \tag{10}$$

where the parameters i and f denote the initial and final states, $\mathbf{e}_\omega$ is the unit polarization vector of the incident photon, ω the light frequency, q the electronic charge, V the volume of the crystal, n the refractive index.

It can be shown that the intersubband transition probability $\eta_{\mathbf{k}}$ may be expressed as[14,16]

$$\begin{aligned} \eta_{\mathbf{k}} &= \frac{2\pi}{\hbar}|M_{fi}|^2 \delta(E_f - E_i - \hbar\omega) \\ &= \frac{B_0 k_z^2}{\omega}\left[\frac{\partial^2 \mathcal{E}_{\mathbf{k}}}{\partial k_z \partial k_x}(\mathbf{e}_\omega \cdot \mathbf{x}_0) + \frac{\partial^2 \mathcal{E}_{\mathbf{k}}}{\partial k_z \partial k_y}(\mathbf{e}_\omega \cdot \mathbf{y}_0) + \frac{\partial^2 \mathcal{E}_{\mathbf{k}}}{\partial k_z \partial k_z}(\mathbf{e}_\omega \cdot \mathbf{z}_0)\right]^2 \delta(E_f - E_i - \hbar\omega) \end{aligned} \tag{11}$$

where B_0 is a constant equal to $\frac{q^2\pi^2}{cVn\hbar^2}$; $\mathbf{x}_0$, $\mathbf{y}_0$, and $\mathbf{z}_0$ are the directional unit vectors.

For an indirect type-II AlAs quantum well layers grown along [110] direction, due to the tilted anisotropic energy band with minimum point away from center, the second partial derivatives $\frac{\partial^2 \mathcal{E}_{\mathbf{k}}}{\partial k_z \partial k_i}$ (i = x, y) can be different from zero. Therefore, it is possible to excite long wavelength intersubband transitions in the quantum well under normal incident illumination. However, for a direct type-I system i.e. GaAs due to the isotropic spherical energy surface and the axis symmetrical parabolic band $E = E_z + \hbar^2(k_y^2 + k_z^2)/2m^*$, it always has $\frac{\partial^2 \mathcal{E}_{\mathbf{k}}}{\partial k_z \partial k_i} = 0$, (where $i \neq z$). The corresponding transition probability becomes

$$\eta_k = \frac{B_0 k_z^2}{\omega}\left[\frac{\partial^2 \mathcal{E}_{\mathbf{k}}}{\partial k_z \partial k_z}(\mathbf{e}_\omega \cdot \mathbf{z}_0)\right]^2 \delta(E_f - E_i - \hbar\omega) \tag{12}$$

Equation (5) reveals that the optical transition would become zero for type-I structures under normal incident illumination. Therefore, it is advantageous for the type-II GaAs quantum well system to have non-zero cross partial derivatives and normal incident excitation of intersubband transitions along [110] growth direction.

It is worthwhile mentioning that the (110) plane is a nonpolar plane with the lowest index in the zinc-blende structure and has been proposed as one of the preferred[17,18] growth orientations for the zinc-blende on diamond systems because of no interface charge imbalance problem exists on this plane. It has also been shown that the layered structures grown along [110] or [111] direction will possess a large built-in in-plane or vertical-to-plane piezoelectric effect, which may lead to a new class of electro-optic devices[19,20].

3.2.3 CONCLUSION

In conclusion, we have demonstrated the first type-II n-multiquantum well LWIPs using an indirect X-band $AlAs/Al_{0.5}Ga_{0.5}As$ system. The desirable normal incident illumination is allowed due to the tilted and anisotropic energy band structure grown on a [110] GaAs substrate. The detector has a peak wavelength at $\lambda_p = 12.8$ μm, and spectral response range of 5.6 to 18 μm. The capabilities of normal incidence, large spectral sensing range, and low device dark current make the present type-II AlAs/AlGaAs LWIP's highly desirable for many infrared applications. Further studies on the interaction effects between the X- and Γ-bands, transition coupling, bandgap engineering, and hot electron transport mechanisms in the type II indirect III-V multiquantum well structures may lead to new and improved infrared detectors, lasers, and modulators.

3.2.4 REFERENCES

1. L. C. West and S. J. Eglash, Appl. Phys. Lett. **46**, 1156 (1985).
2. B. F. Levine, G. Hasnain, C.G. Bethea, and Naresh Chand, Appl. Phys. Lett., **54**, 2704 (1989).
3. G. Hasnain, B.F. Levine, S. Gunapala, and Naresh Chand, Appl. Phys. Lett., **57**, 608 (1990).
4. S.D. Gunapala, B.F. Levine, and Naresh Chand, Appl. Phys. Lett., **70**, 305 (1991).
5. Larry S. Yu, Sheng S. Li, and Y.C. Kao, ***International Electron Devices and Materials Symposium***, pp. 472 (1990).
6. Larry S. Yu, Sheng S. Li,and Pin Ho, Appl. Phys. Lett. **59**, 2712 (1991).
7. Larry S. Yu, Sheng S. Li, Y.H. Wang, and Pin Ho, Appl. Phys. Lett. **60(8)**, 992 (1992).

8. D.D. Coon and R. P. G. Karunasiri, Appl. Phys. Lett. **33**, 495 (1984).

9. A. Kastalsky, T. Duffield, S. J. Allen, and J. Harbison, Appl. Phys. Lett., **52**, 1320 (1988).

10. Larry.S. Yu, Sheng S. Li, Appl. Phys. Lett. **59**, 1332 (1991).

11. Larry S. Yu, Sheng S. Li, Y. C. Kao, *Proc. Government Microcircuit Applications Conference*, Nov. 6 - 8, Las Vegas, Nevada, 479 (1990).

12. Larry S. Yu, Sheng S. Li, Y.H. Wang, and Pin Ho, submitted to J. Appl. Phys., Feb., 1992.

13. E.O. Kane, J. Phys. Chem. Solid **1**, 249 (1957).

14. E. Haga and H. Kimura, J. Phys. Soc. Jpn. **18**, 777 (1963).

15. F. Stern and W.E. Howard, Phys. Rev., **163**, 816 (1967).

16. C. L. Yang, D. S. Pan, and R. Somoano, J. Appl. Phys. **65**, 3253 (1989).

17. H. Kroemer, K. J. Polasco, and S.C. Wright, Appl. Phys. Lett., **36**, 763 (1980).

18. A. Chin, T. Y. Chang, A. Ourmazd, and E.M. Monberg, Appl. Phys. Lett., **58**, 968 (1991).

19. A. Chin, P. Martin, Pin Ho, J. Ballingall, T.H. Yu, and J. Mazurowski, Appl. Phys. Lett., **59**, 1899 (1991).

20. K. W. Gossen, E.A. Caridi, T.Y. Chang, J.B. Stark, and D.A.B. Miller, Appl. Phys. Lett., **56**, 715 (1990).

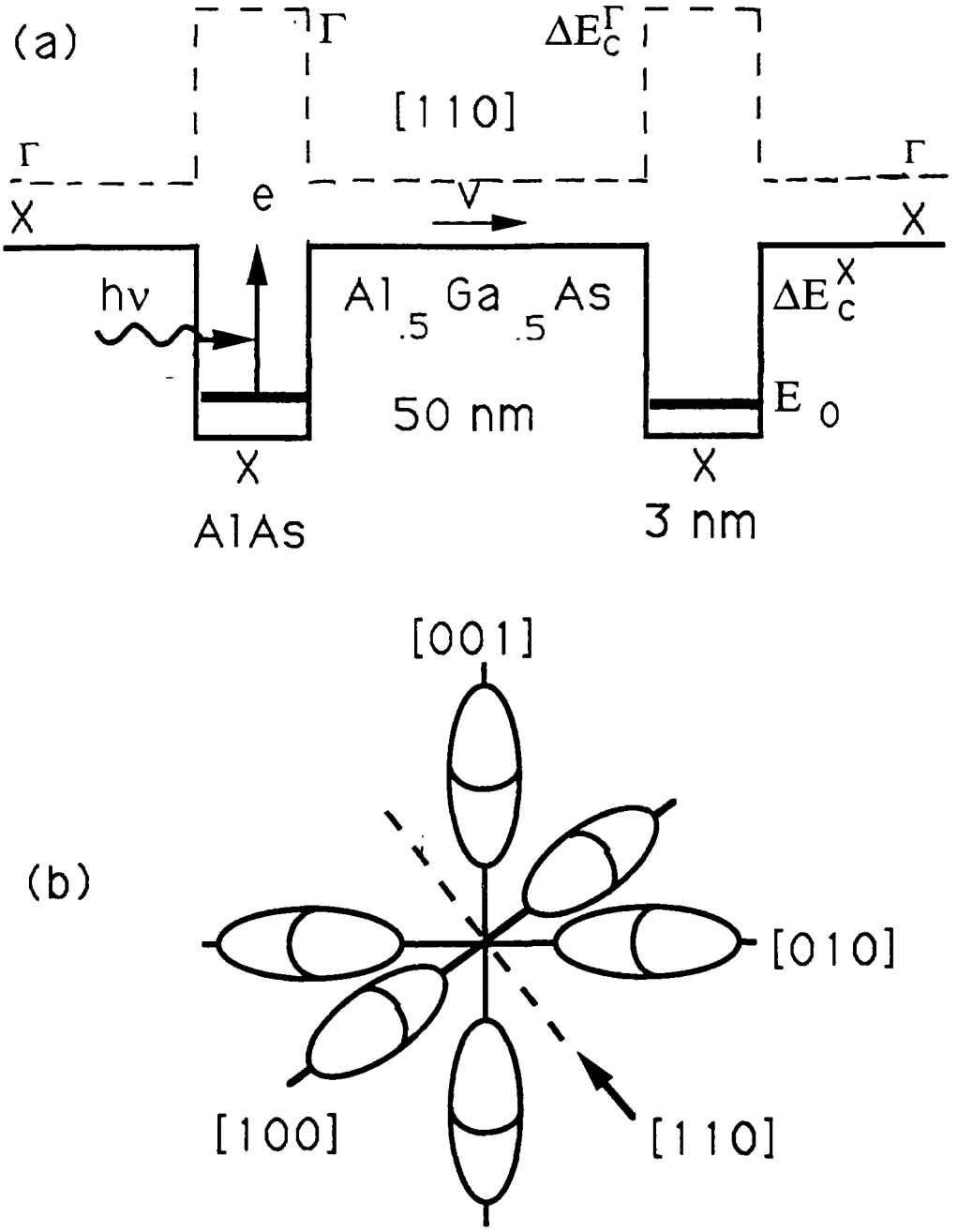

Figure 1 (a) The schematic conduction-band diagram for the type-II $AlAs/Al_{0.5}Ga_{0.5}As$ quantum well infrared photodetectors. The solid lines represent the X-band edge while the dashed lines indicate the direct Γ-band. (b) The six ellipsoids of X-band conduction band minima along [100] axes with centers of the ellipsoids located at about three-fourth of the distance from the BZ center for AlAs. The preferred [110] growth direction is indicated by the arrow.

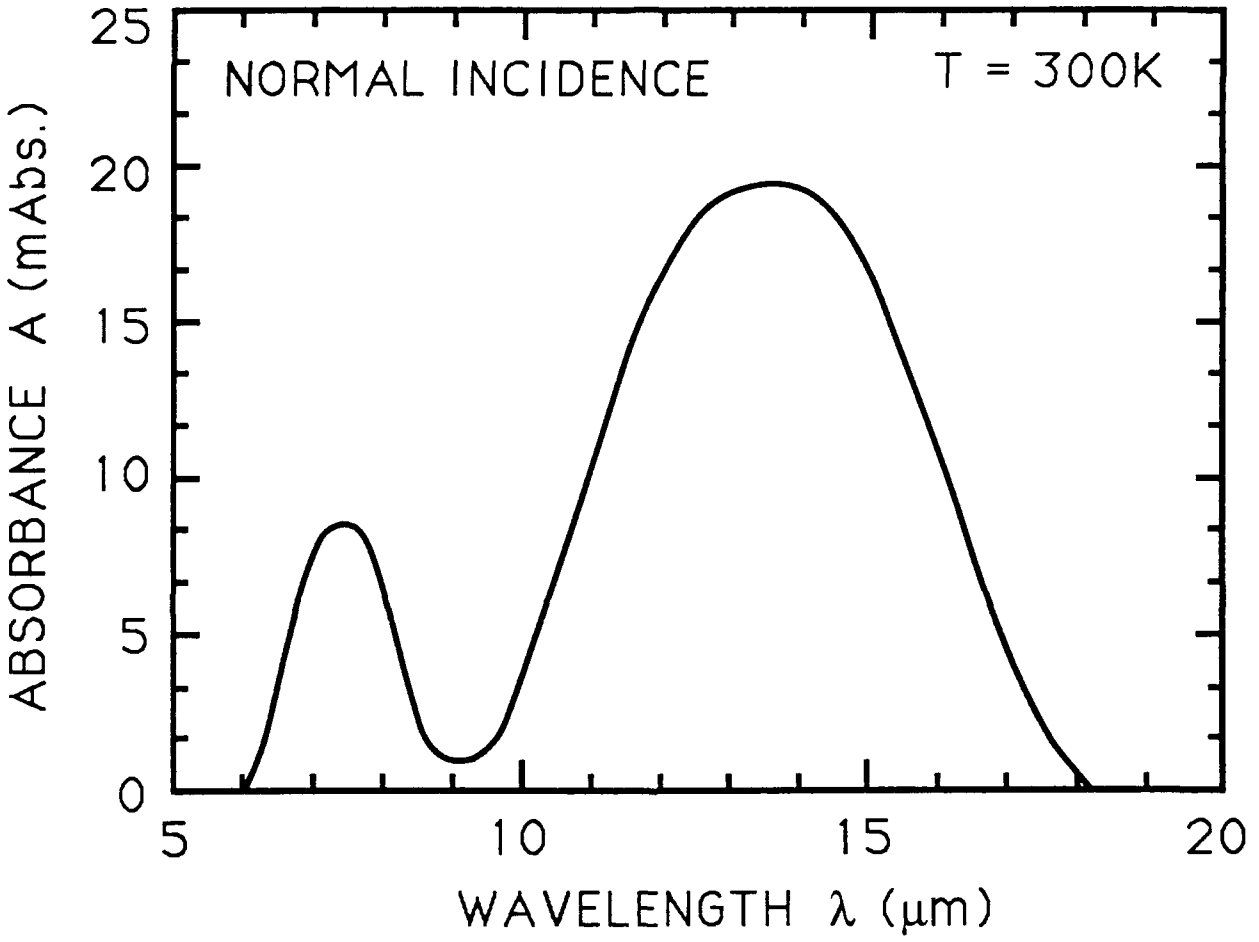

Figure 2 The measured room temperature intersubband absorbance versus wavelength by FTIR spectroscopy at normal incidence.

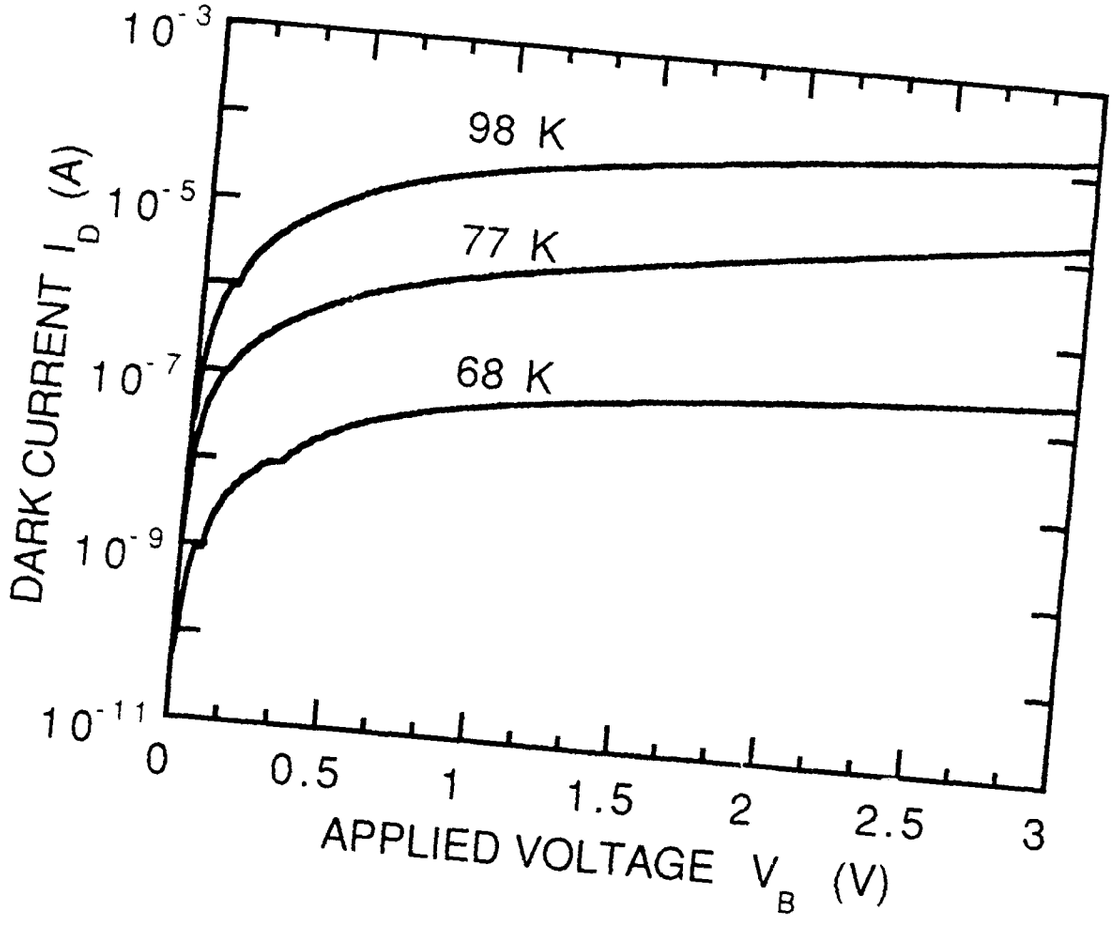

Figure 3 The measured dark current versus applied bias voltage for T = 68, 77, 89 K, respectively.

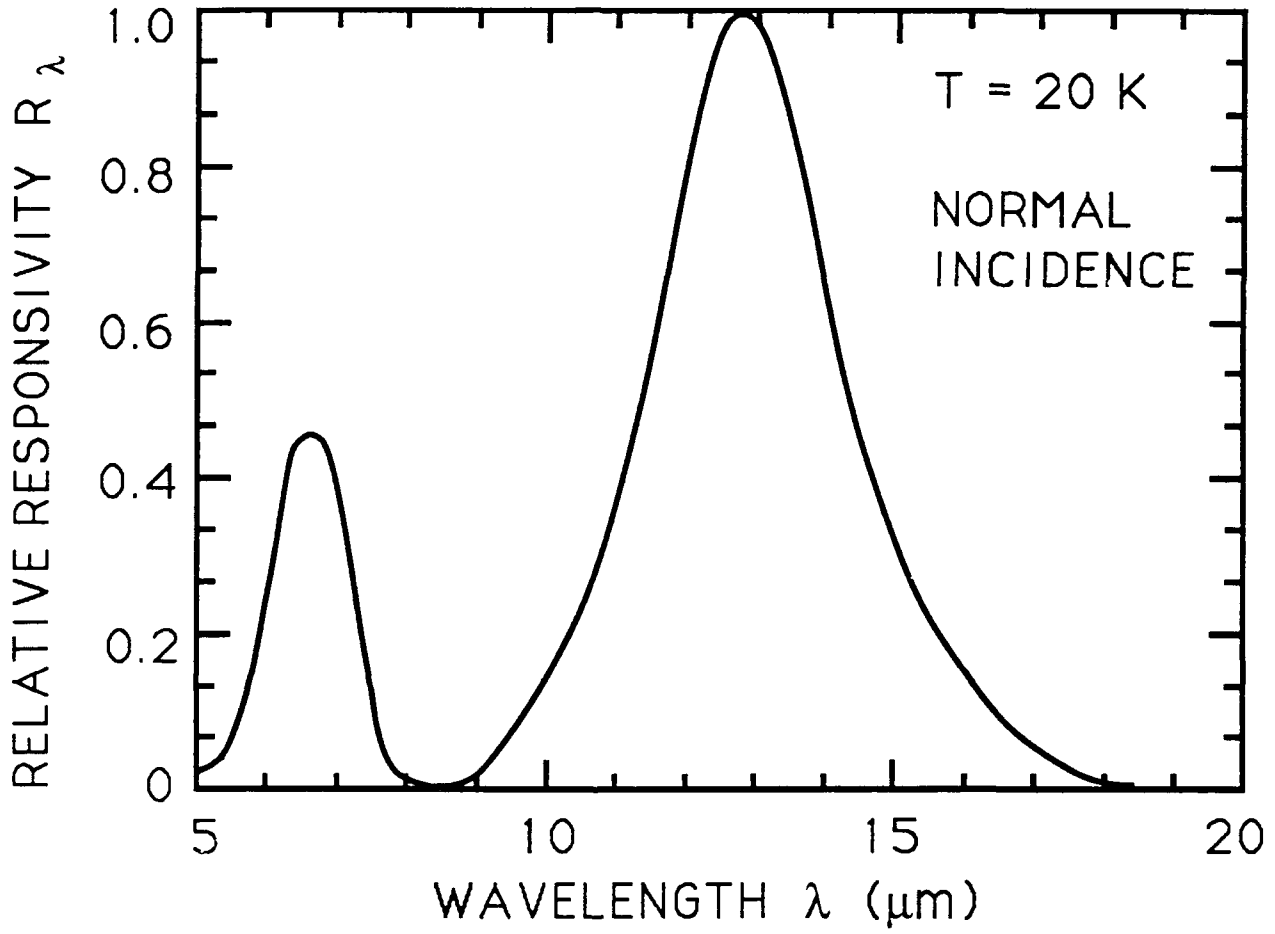

Figure 4 The normalized spectral responsivity measured at V_b = 3 V and T = 20 K